In the early days, Tom and others used a hydrogen maser, which had been calibrated and understood and transported to each antenna. It was used to generate a clock signal. The clock signal from a h-maser is so good, that is good enough to have separate masers at each antenna and the unknown time and the delay needed will be easily taken care of back home at the combining computer. Masers are very expensive. Manufacture and transport of the tapes used in the early system was not an inexpensive addition to the operation. But this allowed Tom Clark, for a long time, to become the world's most accurate geodesist. He mapped plate tectonics, changes in flows and currents in the world's oceans, and could even see El Niño and measure it before others could based on the rate of change of the rotation of the Earth using the system he ran for NASA.

In the next figure, we will see most of the elements of this system. This system is the modernized one. Rather than expensive tapes, much less costly to acquire, deploy, return to home base and consume the data are hard drives. The density of data on them, the physical reliability of them, and the steadily decreasing weight, power, and number of moving parts have made them the mainstay of transporting petabytes of data around the world. Next, Tom, with help from others, developed the Totally Accurate Clock (TAC - also Tom's initials) and developed it into a GPS or GNSS disciplined oscillator and clock. This replaces the hydrogen maser in many different applications. TAPR sold the TAC kit for a long time and Rick Hambly, W2GPS, operates a successful business at CNS Systems, Inc., around the concepts in the TAC.

In Figure 2, you can see the GNSS system, the VLBI sampler, and recorder at each of the antennas. The VLBI correlator is "home base" computer where all the data is assembled and analyzed. Tom became the leader of the team that was the world's most accurate geodesists using this system, and as in the figure, his signal of interest was from the quasars, as depicted. They provided the common signal of interest used by all the antennas in the array.

Event Horizon Telescope (EHT)

The ideas demonstrated in the previous picture are the basis for the EHT. They are at the heart of the system. Astronomers like to make images to quickly get a look in a useful way at the data collected. Lots of brilliant work has gone into cleaning up the data, figuring out how to patch holes in the coverage on the sky and in the objects of interest (CLEAN, etc.), and achieving excellent resolution in the images that are now being shown. This includes a form of super resolution derived by training neural network models (deep learning) to take the really good, but still fuzzy images, and automatically answer the question: If I see this fuzzy image, which is my best estimate of the picture underneath it if I had much better resolution than I have now? Lots of data and lots of physics go into calculating the "high resolution" version of these pictures to train the neural networks to work reliably. And, in the end, you get the world's first image of the event horizon of a 6.5 billion solar mass black hole in another galaxy. It is simply amazing as is the next figure.

This donut is a miracle of modern science and engineering, and is the latest proof that Einstein is one of the greatest minds of all time.

Last Word On This

One can never know where one's work will lead. And even the smallest contributor to major efforts is a benefit to humanity. Examples include the achievement of landing humans on the moon and returning them safely, finding the last remaining predicated particle in our knowledge of the microscopic universe governed by quantum mechanics at the Large Hadron Collider, called the Higgs Boson, which is proof of the conjecture that the Higgs field is real (and badly needed since it is responsible for us having mass and not being a bundle of things flying around at random at the speed of light) and confirm the "Standard Model" of physics not including gravity. And finally, to have contributed in a major way to the science and engineering of VLBI for a career that was the underpinning of the event horizon picture of the supermassive black hole at the center of the Messier Object, M87, a galaxy in the Virgo galaxy cluster. M87 is easily visible in amateur telescopes that you can use in your back yard. The work of Tom Clark and many others enabled us to build a telescope the size of the Earth and see Einstein's second weirdest creation, a black hole. Who knows Einstein's first weirdest creation? It has nothing to do with gravity. He discovered entanglement and brought us all the weird wonders and applications that this will bring. My last remark is thank you, Tom, for mentoring and involving so many people in your endeavors.

Reference

Thompson, A.R. et. al. *Interferometry and Synthesis in Radio Astronomy* (Third Edition), Springer, Astronomy and Astrophysics Library.

RF Generator Techniques for Space Applications

Jurgen Vanhamel, ON5ADL
jurgen.vanhamel@aeronomie.be

A deeper insight into the performance of a Hilbert transform and PLL-based generation technique for space missions

The use of an RF generator is quite common in lab testing environments as well as in commercial applications. Many different RF generation techniques exist, both analog and digital. The frequency domain sets the complexity of the circuit. It is commonly accepted that the higher the frequency, the more complex the design becomes. Designing for space applications change things quite drastically. Elements as survivability, radiation and redundancy also come into play. Taking into account that adaptations are not any longer possible after launch, implies that the implemented design has to be one hundred percent robust. The complexity rises when designing for scientific missions like for NASA or ESA because of the more severe imposed constraints. This article tries to give an idea about how to design a pure sinewave RF generator at rather low frequencies (< 500 MHz) for a scientific mission capable of surviving under the harsh environmental conditions of space, dealing with the space agency restrictions and limited availability of approved electrical components.

1. Designing for space

Designing for space applications forces the engineers to use techniques which sometimes look a little bit odd. The reason for this is the lack of available and approved components for space. While designing for space, the first thing that needs to be checked is if the components used in the proposed design have space qualified counterpart. The design based on commercial devices needs to be transferrable into a space-grade version. This limits the search for components drastically. Not all commercial components have a space-grade version available. Different qualification levels for components exist like V-class or Q-class, depending on the orbit or mission for which these devices are going to use. Also, military grade components exist, but in most cases, the resistance against radiation and shock is not high enough for use in space.

A space grade model of a component will

be subjected to a suite of environmental tests such as thermal-vacuum, vibration, radiation, shock and Electromagnetic Compatibility (EMC). Also, the foreseen lifetime of the mission and the selected orbit around the earth (or beyond) has an impact on the design process. Besides the selection of components, also the PCB-design and manufacturing have to be done following space qualified standards. Working for ESA, for instance, implies that the designer has to follow the so-called ECSS-standards[1]. These rules describe meticulously what can and can't be done in the design work. Besides that, power and mass limitations, voltage restrictions on the available supply lines and PCB (Printed Circuit Board) area limitations are other vital parameters influencing the design.

2. RF generation techniques

Taking into account all restrictions listed in the previous paragraph, still, several different RF generation techniques are feasible. The signal can be produced digitally and converted into an analog form or generated in a pure analog way. For this article only two analog pure sine wave generation techniques are being discussed, namely the Hilbert transform technique and the PLL-technique (Phase Locked Loop). Both are composed of commercial-grade components, but having a space-grade counterpart available on the market.

2.1 The Hilbert transform technique

This technique is a rather old way of generating an RF signal[2]. The Hilbert transform principle (see Figure 1) splits the input signal m(t) into two chains from which one chain is shifted by 90° in phase. Additionally, a local oscillator is split into two chains. Again one part is shifted by 90° in phase. These two chains produce two parts of the signal namely 0.5 Ac sin(-c t) and 0.5 Ac cos(-c t). Combining each signal with the input signal m(t) into a mixing circuit creates two shifting output chains. One in which a phase shifting occurred and another in which no phase shift is done. Both outputs chains are combined into a summing device creating a USB (Upper Side Band) and LSB (Lower Side Band) signal s(t), depending on the mathematical operation.

The practically implemented concept of the Hilbert transform to build an RF generator is shown in Figure 2. The core of this technique is a space qualified reference oscillator linked to a space qualified Actel-Microsemi RTAX-FPGA (Field Programmable Gate Array) [RTAX2000S-CQ352V (V-flow)[3]]. The

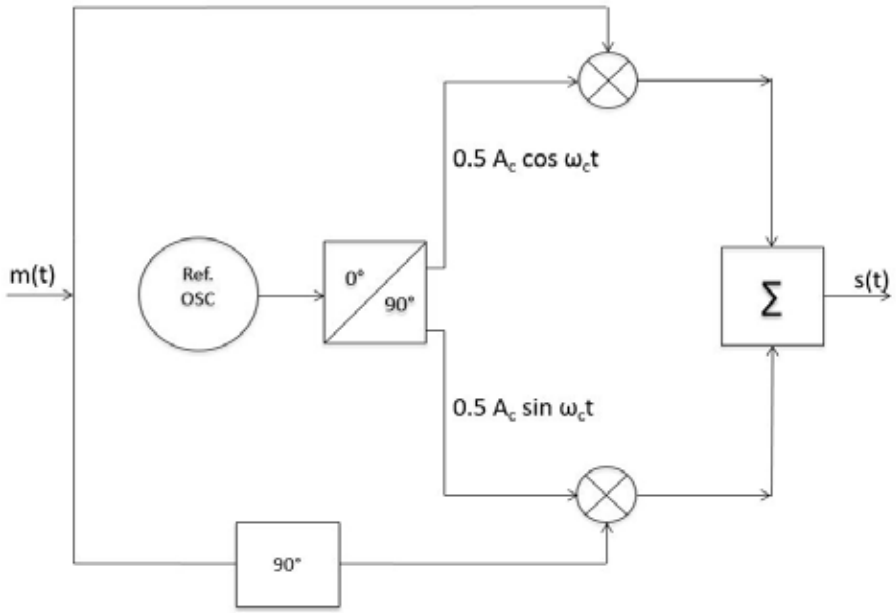

Figure 1 — Hilbert transform setup.

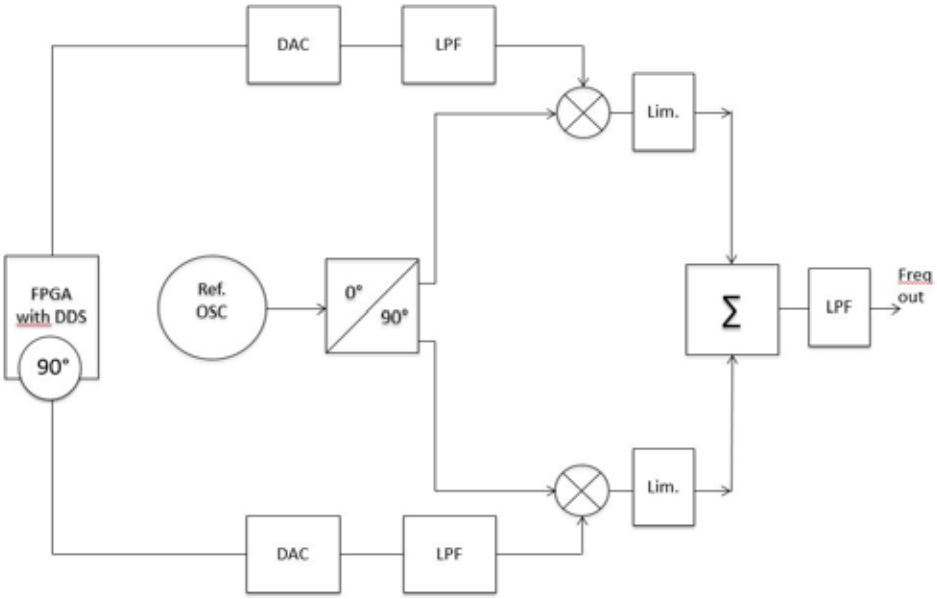

Figure 2 — Practical implemented Hilbert transform setup for an RF generator.

selected FPGA, one of the few available on the market for space applications, is a one-time programmable device, capable of withstanding a high level of radiation. This device consumes around 1 W and runs at a frequency of 127 MHz. Inside this FPGA a DDS (Direct Digital Synthesis) is programmed in VHDL to generate a pure digital sinewave in the desired frequency range. The output signal is fed to a space qualified DAC (Digital to Analog Converter) of Texas Instruments[4] on one side and 90° shifted and fed to another DAC on the other side of the setup. Both outputs of the DACs need to be filtered in an adequate way to remove all spurs and harmonics to achieve a pure sinewave. The phase of the output signal of the reference oscillator is shifted in one track by 90°. Both signals are applied to two mixers, combing the oscillator outputs of the DACs and reference oscillators. A summing device, together with an additional low pass filter, combine the two chains to produce the final output signal. All components used in this Hilbert setup are available in a space-grade and commercial version.

To proof the concept a commercial fixed oscillator of 90 MHz was used, together

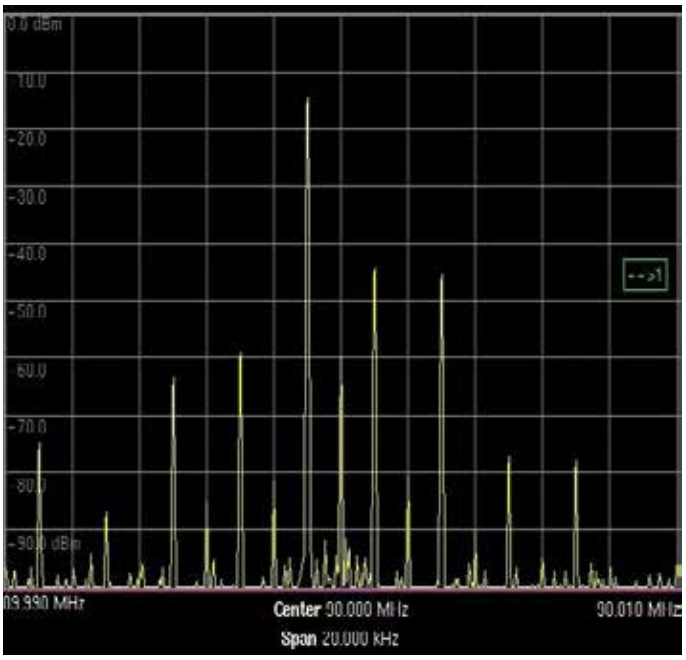

Figure 3 — Spectrum of the combination of 90 MHz and 1 kHz LSB.

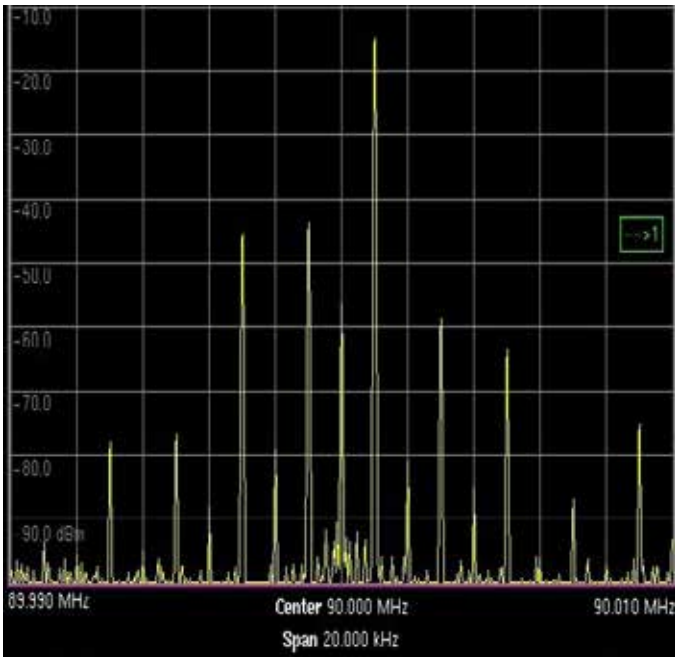

Figure 4 — Spectrum of the combination of 90 MHz and 1 kHz USB.

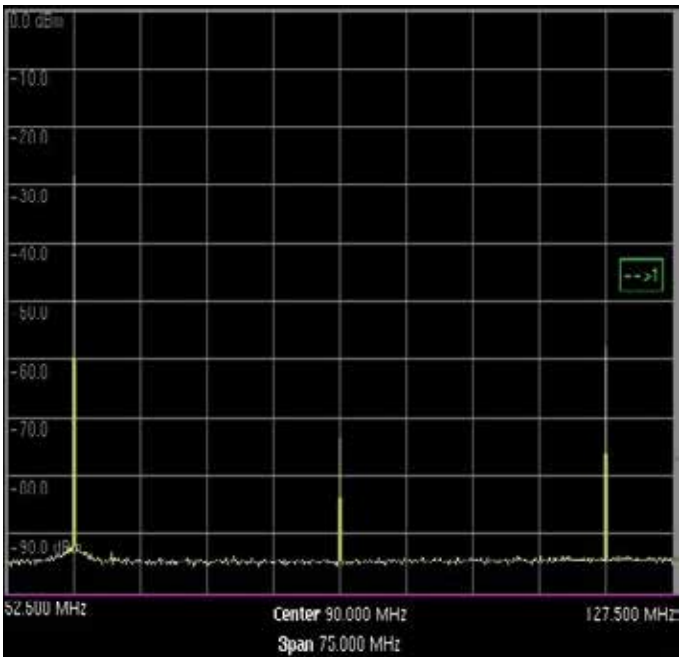

Figure 5 — Spectrum of the combination of 90 MHz and 30 MHz LSB.

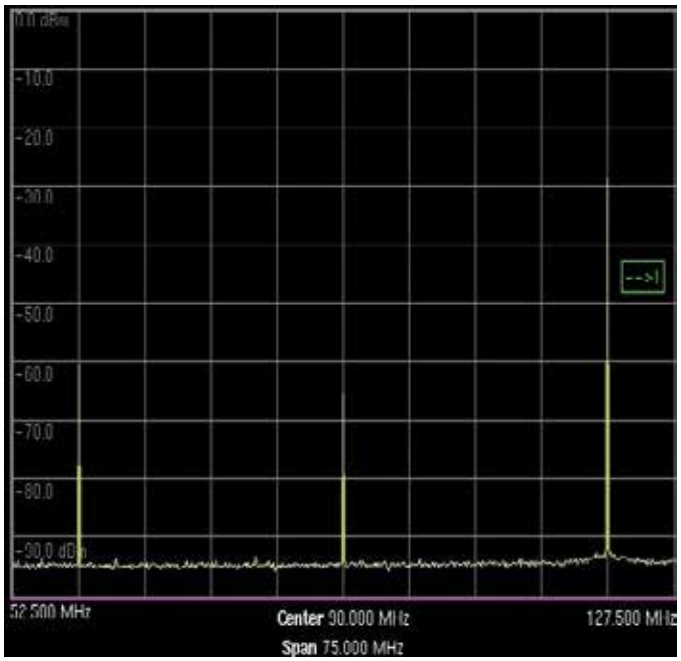

Figure 6 — Spectrum of the combination of 90 MHz and 30 MHz USB.

with a programmed frequency in a DDS-DAC combination between 0 and 30 MHz, leading to a sinewave with an output frequency between 60 MHz (= 90 MHz – 30 MHz) and 120 MHz (= 90 MHz + 30 MHz). All in-between frequencies can be generated by selecting another driving frequency in the DDS. The produced spectrum in Figure 3 highlights an output frequency of 90 MHz with an LSB at 1 kHz. In Figure 4, the same 90 MHz signal is created with a USB of 1 kHz. Additionally, in Figures 5 and 6, the lower range of 60 MHz and the upper range of 120 MHz is shown. It is clear that the output signal around 90 MHz has an amplitude of -12 dBm, whereas at the borders of the frequency range this falls back to less than -28 dBm. This means significant amplification of the output signal is needed. It is clear that many spurs and harmonics are generated, depending on the used frequency setting. The origin lays in the combination of several mixing circuits and the summing at the end of the chain. The difference between the desired signal and the first undesired spur is around – 30 dBc which is a common requirement in space generation techniques. A solution can be the limiting of the signal at the end of the chain, directly after the summing device.

By selecting different reference oscillator values and DDS ranges, other output frequencies can be covered. For instance, using a reference oscillator of 45 MHz and a DDS covering between 0 and 15 MHz a

frequency range can be generated between 30 MHz (= 45 MHz – 15 MHz) and 60 MHz (= 45 MHz + 15 MHz). The only limitation here is to create a DDS inside a space qualified (and approved) FPGA that can generate a broad frequency range. Additionally, a space qualified reference oscillator with a frequency that can cover the needs has to be found. For the approved RTAX device the maximum DDS-DAC output frequency is about 60 MHz taking the Nyquist theorem into account. Combining this with for instance a 90 MHz reference oscillator would create an output frequency between 30 MHz and 150 MHz. Of course, the filtering of the output signal after the DAC will be a major issue in this case.

As shown in Figure 2, the number of building blocks is high. Also, the consumed power of 1 W for the FPGA and two times 600 mW for the DACs is not negligible. Another impact of using more building blocks is the rise in mass, complexity and used volume on the PCB. The positioning of the blocks has to be done intelligently not to destroy the PCB during launch due to shocks and G-forces imposed by the launch vehicle. The kind of launcher will impact these parameters as well because each vehicle has his key properties.

2.2 The Phase Locked Loop technique

This fully analog technique is widely used in commercial applications for telecommunication. Also, many telecommunication satellites use this setup to generate a stable pure sinewave RF signal in a rather high-frequency range (above 1 GHz). The general idea of a PLL is to use a feedback loop to constantly correct the frequency of the output signal by comparing the phase of a stable reference oscillator signal with the generated output signal of a VCO (Voltage Controlled Oscillator). The general concept is shown in Figure 7. Based on the phase difference between f_{REF} and f_{DIV} an error signal is generated by the PFD (Phase and Frequency Detector) as a pulse width modulated signal. The width of the pulses is determined by the magnitude of the measured phase difference. This signal is fed into a charge pump mechanism to generate constant current pulses. Additionally, a loop filter (active or passive) is used to convert the current pulse train into a continuous voltage capable of driving the VCO into the requested output frequency (f_{OUT}). The combination of a charge pump and PFD significantly reduces the settling time of the PLL loop due to the independence of the requested frequency and generated frequency. The difference between these parameters is measured directly via the phase difference.

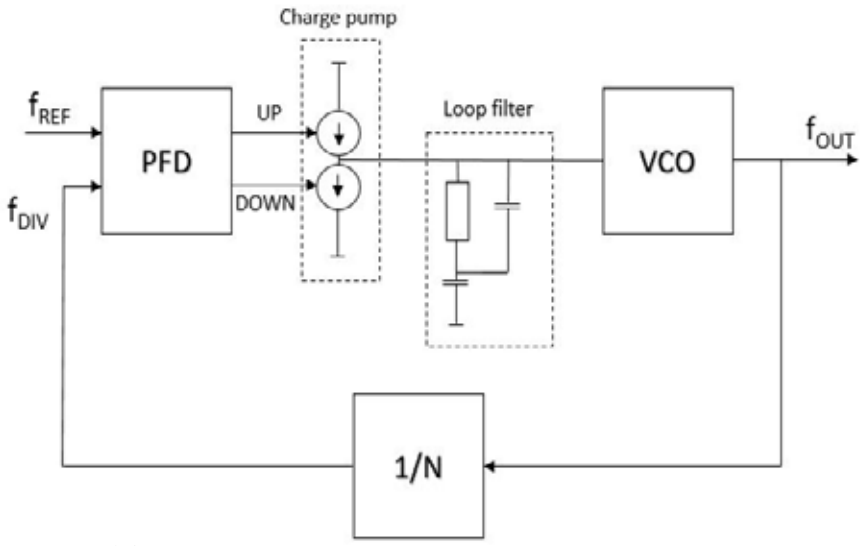

Figure 7 — The general PLL concept.

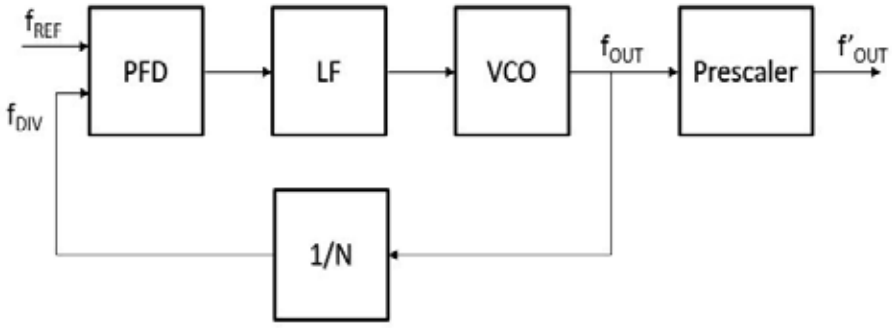

Figure 8 — An adapted space qualifiable PLL concept to run at lower frequencies (< 500 MHz).

Figure 9 — Picture of the assembled PCB containing the PLL chain, power handling and PIC.

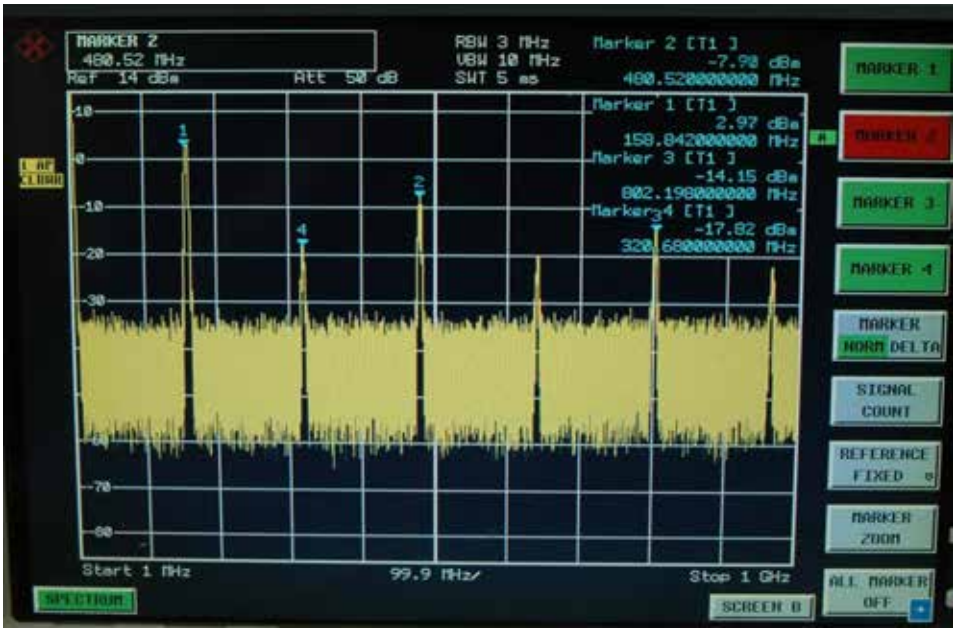

Figure 10 — Spectral output @ 1 GHz VCO frequency.

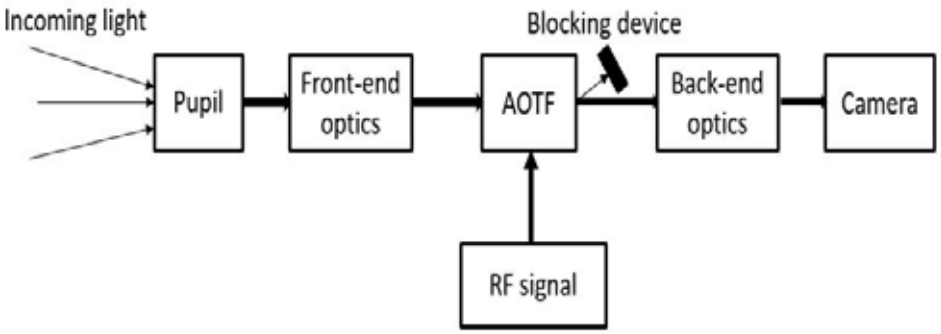

Figure 11 — ALTIUS space mission concept.

Figure 12 — Limb of the atmosphere.

On the contrary, the use of a charge pump introduces glitches caused by imperfections in the two UP and DOWN signals in the charge pump itself. Besides the integration function of the loop filter, it is also capable of eliminating these glitches. The choice of loop filter significantly influences PLL chain key parameters such as bandwidth, spurious emissions and noise.

The loop filter can be active or passive. The concept of a passive filter is easier to implement and requires less board area compared to an active setup. An active loop filter is used in case the tuning voltage range of the VCO exceeds the capabilities of the frequency synthesizer. An active loop filter setup is capable of driving the VCO into a higher tuning range so that a VCO with a broader output frequency range can be used. Both filter concepts work as an integrator on the incoming signal.

The use of a PLL makes it possible to generate a broad range of frequencies. In telecom mostly a high range of frequencies is required in ground-based as well as space-based applications. In scientific missions, interests go rather to lower frequencies, preferably below 500 MHz. For this, it is not so convenient to find suitable space qualified components, especially a dedicated VCO. So the idea was to generate a rather high frequency in the PLL and additionally downscale this frequency to a lower range by the use of prescalers. A possible general setup of this idea is shown in Figure 8.

In the described example a VCO is used in the frequency range between 1 and 2 GHz. Teledyne has several space grade products on the market[5]. For the tests, a commercial model of this device was not available at that time (due to lead time in the production), so a commercial alternative of Minicircuits was used, namely the ZX95-2500W+[6]. Of this device, no space grade counterpart exists, but the space grade models available by Teledyne have comparable properties. A frequency synthesizer of Analog Devices[7] is used to compare the two signals. The output frequency is additionally downscaled by the use of two cascaded prescalers (divide-by-8 and divide-by-2) to a range between 62.5 MHz and 125 MHz. No direct divide-by-16 prescaler suitable for space exists. By adapting the prescaler value, other frequency ranges can be generated. Different prescalers are available as space qualified components by Teledyne/E2V/Peregrine[8].

To perform the programming of the frequency synthesizer, a PIC microcontroller (PIC18F46J50) of Microchip[9] is used

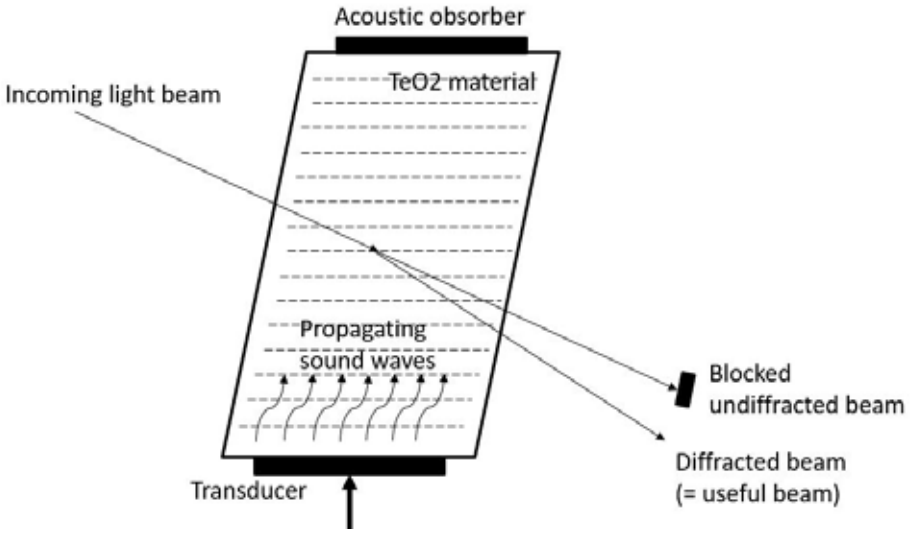

Figure 13 — Acousto-Optical Tunable Filter concept.

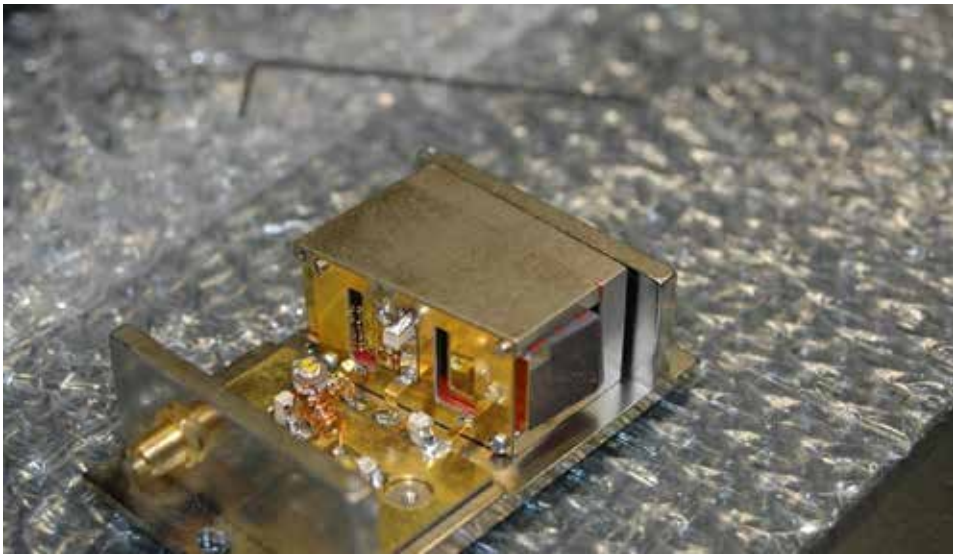

Figure 14 — Acousto-Optical Tunable Filter used by the author.

together with an own build GUI (Graphical User Interface). This device is not suitable for space, but many space grade microprocessors exist capable of performing the same task.

The complete assembly of the PLL can be seen in Figure 9. On the left, the assembled PLL chain is shown, including the prescalers and power handling part is included. The latter is mostly separated in space grade RF generators but is currently integrated onto the PCB using non-space grade components for test purposes. On the right, the microcontroller can be seen. The generated output spectrum can be seen in Figure 10. It is clear that the generated signal has a higher amplitude (+2.97 dBm) compared to the Hilbert transform based generation technique. Also, the amount of generated spurs and harmonics are less, and the amplitude is lower. For example, the second harmonic is -20 dBc without any filtering.

The power consumption of this RF generation technique is around 2 W in total. Also, less building blocks are used which means the design can be compact which is very important for space applications due to the limited space available in payloads.

3. Space mission applicability

This paper gave an overview of two possible RF generation techniques suitable for space applications. Currently, the PLL technique is proposed as an RF generation technique for an ESA (European Space Agency) space mission called ALTIUS[10] (Atmospheric Limb Tracker for the Investigation of the Upcoming Stratosphere). The concept of the instrument consists of three separate independent channels, each observing the atmosphere in a different wavelength domain, namely in the ultraviolet (250 nm to 450 nm), visible (440 nm to 800 nm) and near-infrared (900 nm to 1800 nm). The visible and near-infrared channel is built according to the concept shown in Figure 11. Light enters the front end optics, and additionally, a filter mechanism selects the desired wavelength. Further, the back end optics focuses the image onto a camera at the end of the channel. The camera is capable of making images of the limb of the atmosphere (see Figure 12). By mathematically analyzing the captured images, the concentration profile of different gases like ozone, greenhouse gases and others can be monitored related to a height profile.

The RF generator is used to select the different wavelengths by driving an AOTF (Acousto-Optical Tunable Filter). This device is a sort of SAW-filter (Sound Acoustic Wave) capable of using RF to select different optical wavelengths[11]. In Figure 13 the concept of the device is explained, while in Figure 14 a practical device, used by the author, can be seen. A more detailed explanation of this device would lead too far, but the principle is based on birefringent interaction inside the device itself. An RF signal is applied to a transducer which is mounted on the side of the device. The transducer converts the RF into sound which propagates through the crystal. For each different RF frequency, a different soundwave propagates through the crystal, which makes another optical wavelength coming out of the AOTF. A specific mechanism blocks the undiffracted beam. By this, different wavelengths can be displayed onto the detector at the end of the instrument. By analyzing the captured image, different concentration profiles can be composed, related to the altitude above ground level.

4. Conclusion

This paper tried to give a non-exhaustive overview of possible RF generator techniques applicable for (scientific) space missions (imposed by agencies such as ESA and NASA) with a primary focus on generating a pure sinewave at rather low frequencies usable in scientific space-related missions. Based on the two investigated techniques, it became clear that the PLL technique has more advantages compared to the Hilbert transform technique. Less power, fewer harmonics and spurs, and less building blocks imply that the PLL technique is the preferred solution out of the two. Both

techniques are transferable into space grade designs. Designing for space is clearly limited by the availability of space grade components and constraints which can lead to the use of sometimes rather strange techniques.

Notes

[1] ESA ECSS standards for space missions, **ecss.nl/standards/**.

[2] P. Das, D. Shklarsky and L.B. Milstein, "SAW implemented real-time Hilbert transform and its application in SSB, *IEEE Ultrasonics Symposium, 1979*, pp 752-756.

[3] The Actel RTAX FPGA, RTAX2000S-CQ352V (V-flow), **www.microsemi.com/products/fpga-soc/radtolerant-fpgas/rtax-s-sl9.**

[4] Texas Instruments Digital to Analog Converter, DAC5675A-SP.

[5] Minicircuits ZX95-2500W+ VCO, **194.75.38.69/pdfs/ZX95-2500W+.pdf.**

[6] Space grade products of Teledyne; **www.teledynemicrowave.com/index.php/teledyne-microwave-space/microwave-solutions-space.**

[7] Frequency synthesizer of Analog Devices (1 – 7 GHz) ADF4180(S); **www.analog.com/media/en/technical-documentation/data-sheets/adf4108.pdf** (commercial version) and **www.analog.com/en/products/clock-and-timing/phase-locked-loop/integer-n-pll/adf4108s.html** (space grade model).

[8] Teledyne/E2V/Peregrine prescalers; **www.e2v.com/products/semiconductors/peregrine/.**

[9] The PIC microcontroller (PIC18F46J50) of Microchip; **ww1.microchip.com/downloads/en/DeviceDoc/39931b.pdf.**

[10] E. Dekemper et al., "ALTIUS: a Spaceborne AOTF-based UV-VIS-NIR Hyperspectral Imager for Atmospheric Remote Sensing," *Proceedings Of SPIE*, 9241-92410L(1-10), 2014.

[11] I.C. Change, "Noncollinear Acousto-Optic Filter with Large Angular Aperture," *Applied Physics Letters* 25, 1974, pp. 370-372, doi: d**x.doi.org/10.1063/1.1655512**.

Bibliography

Jurgen Vanhamel – ON5ADL – received his call in 2002 (formerly ON1ADL). He has a bachelor degree in mathematics, a master degree in industrial sciences (electronics), a postgraduate in avionics and spacionics and holds several courses in aeronautical subjects. He is currently working on his Ph.D. He works as a project engineer at the Belgian Institute for Space Aeronomy in Brussels – Belgium. He is responsible for a space mission as well as several other ground-based projects. Besides that, he is also active as a radio amateur and interested in amateur satellites, propagation predictions and SDR.

DM31 Activation, Organ Pipe Cactus National Monument

Patrick Stoddard, WD9EWK/VA7EWK

Among satellite operators who are interested in confirming contacts with the 488 grids making up the continental USA, grid DM31 is one of the rarest grids. Most of DM31 lies in Mexico, where there aren't any operators working satellites or any VHF/UHF bands. The northeast corner of DM31 extends into southern Arizona around the Organ Pipe Cactus National Monument and the town of Lukeville. For most who wish to operate from DM31, the Arizona portion of the grid is the destination for any grid expeditions. I have done this several times since 2009, doing my part to put this grid on the satellites. On 2 February 2019, a Saturday, I made another excursion out to DM31 for a day of satellite operating. This was my first trip to DM31 in almost a year after my last trip in mid-February 2018, and it was the busiest of any of my DM31 trips.

Before going on the road, I prepared a list of passes I could work from DM31 on satellites in FM, SSB, and packet. AO-85 had been back in operation for a few days, meaning all 4 FM satellites should be available for passes. With the CAS-4 and XW-2 satellites, there was no shortage of passes I could work in SSB. FalconSat-3 passes were happening during the daytime, and a pleasant surprise happened while I was in DM31 - the ISS digipeater was active once again, after several weeks of being unavailable. I made sure I had the right mix of radios to work all of these passes... an Icom IC-2730 dual-band mobile radio for the FM satellites, a pair of Yaesu FT-817NDs for SSB, and two different radios for the packet digipeaters (Kenwood TH-D72 for FalconSat-3, Kenwood TH-D74 for the ISS), and an Elk log periodic antenna. I packed a lunch, since the options for getting a meal out there are few - a convenience store and restaurant at the border, or other convenience stores and a small casino about 25 to 30 miles to the north. The nearest fast-food restaurant was over an hour away to the north, at Gila Bend along Interstate 8.

The Organ Pipe Cactus National Monument is in southern Arizona, a 2.5- to 3-hour drive from the Phoenix area. I had initially planned to get out to DM31 around 9am (1600 UTC), in time for an AO-92 pass. The list of passes I prepared showed a SO-50 pass just after 1430 UTC, a pass favoring the eastern half of the continental USA. With this in mind, I changed my departure time to around 1200 UTC.

With no traffic around Phoenix at that hour on a Saturday morning, and no rain to slow traffic on the way to DM31, I made the drive to DM31 in about 2.5 hours. I parked near the national monument's visitor center a few miles north of the U.S./Mexico border and had a few minutes to prepare for that SO-50 pass. I took some pictures of the radio and antenna on my car, along with a GPS receiver to document my location. When SO-50 came up over the hills to the north,

The author's portable station: 2 Yaesu FT-817NDs, Kenwood TH-D74 and TH-D72, ICOM- 2730, Elk log periodic antenna.